U.S. DEPARTMENT OF COMMERCE
NATIONAL OCEANIC AND ATMOSPHERIC ADMINISTRATION
NATIONAL WEATHER SERVICE
NATIONAL METEOROLOGICAL CENTER

OFFICE NOTE 387

A MIXED LAYER MODEL OF THE UPPER OCEAN COUPLED TO THE MEDIUM RANGE FORECAST MODEL (MRF-91)

STEPHEN BRENNER
UCAR VISITING SCIENTIST

AUGUST 1992

THIS IS AN UNREVIEWED MANUSCRIPT, PRIMARILY INTENDED FOR INFORMAL EXCHANGE OF INFORMATION AMONG NMC STAFF MEMBERS

Abstract

A mixed layer model of the upper ocean was developed and coupled to the global Medium Range Forecast model (MRF-91). This model is of the type commonly referred to as bulk models and includes detailed parameterizations of wind mixing, convective overturning, heating and cooling by surface fluxes, heating by penetrative radiation, and large scale vertical advection driven by the curl of the wind stress. The model was tested under a series of idealized forcing cases and the results compared favorably with those of similar models.

The mixed layer model was then coupled to the MRF-91 and run once every 12 hours right after the radiation computations. The coupled model was tested in both one way and two way interaction modes. In the former, the ocean model was forced by the MRF surface fluxes but the predicted sea surface temperatures (SST) were not fed back into the MRF. In the two way mode, the two models were fully interactive with predicted SSTs at each ocean model time step used in subsequent surface flux computations. Results from a 10 day forecast were quite encouraging. The large scale pattern of SST changes was generally predicted quite well with predicted changes somewhat smoother and smaller than observed. There were also several significant deficiencies such as an underestimate of cooling in the Southern hemipshere. Nevertheless, compared to the current operational "no-change" SST prediction, the coupled model SST changes are clearly superior and skillful.

1. Introduction

In the present NMC global medium range forecast system, sea surface temperatures (SST) are held fixed throughout the forecast period with values taken from the SST analysis at the initial time. Several studies (e.g., Ranelli et al., 1985) have indicated that the impact of daily changes of SST on medium range forecasts is quite variable. However this insensitivity could be linked to the limited amount of variability contained in the analyzed SST fields used for updating during the forecast since these SST fields are generally averaged over periods ranging from 5 to 14 days. This insensitivity may also be linked to deficiencies in the surface flux computations of the particular atmospheric model in use. On the 30-90 day time scale, the response of the forecasts to changes in SST is more clearly defined (e.g., Owen and Palmer, 1987; Michaud, 1990) with the use of analyzed SST having clear advantages over the use of climatological SST. When performing hindcast experiments the SST analyses are readily available. However in a forecasting mode the only possible way to update SST (other than climatological changes) is through the use of an ocean model.

As a first step in assessing the potential impact that updating SST may have on 10-30 day operational forecasts, a one dimensional, variable depth mixed layer model of the upper ocean was designed and coupled to the MRF-91. In addition to the potential for improved predictions, this type of experiment provides a powerful tool for assessing the strengths and

weaknesses of the MRF computed surface fluxes.

In the next section we describe the mixed layer model in detail. In section 3 we describe the results of tests of the mixed layer model with idealized forcing and in section 4 we describe the strategy for coupling to the MRF along with results from some experimental 10 day forecasts. In section 5 we present our conclusions and recommendations for further research.

2. Mixed layer model

The mixed layer model of the upper ocean used for this study is an extension of the model described by Brenner et al. (1991). It is based on the conservation equations of heat and salt

$$\frac{\partial \bar{T}}{\partial t} + \bar{w}\frac{\partial \bar{T}}{\partial z} = -\frac{\partial}{\partial z}\overline{w'T'} + \frac{1}{\rho c_p}\frac{\partial I}{\partial z} \qquad (1)$$

$$\frac{\partial \bar{S}}{\partial t} + \bar{w}\frac{\partial \bar{S}}{\partial z} = -\frac{\partial}{\partial z}\overline{w'S'} \qquad (2)$$

where T and S are temperature and salinity at depth z (increasing downward), t is time, w is the vertical velocity, I is the penetrative component of solar radiation, ρ is density, c_p is the specific heat, and an over bar ($\bar{}$) and prime ( )′ are the mean and turbulent components. The second term on the left hand side of each equation is the vertical advection by the mean flow while the first term on the right hand side represents the

effects of turbulent transport. The model is completed by an equation of state which relates density, temperature, and salinity. Equations (1) and (2) are solved numerically with a forward in time and centered in space scheme.

2.1 Turbulent transport

The turbulent transport or Reynolds stress terms in (1) and (2) are used to represent the effects of three distinct mixing processes: free convection due to static instability, forced convection due to wind mixing, and all other subgrid scale vertical mixing processes.

Free convection is caused by cooling at the surface by the net heat flux and is the major process responsible for the deepening of the mixed layer in fall and winter. In our model, an instability is removed by mixing the unstable layer with the layers below as necessary to restore a neutral density lapse rate (e.g. Bryan et al., 1975). The mixing is assumed to be instantaneous and to completely mix temperature and salinity.

Forced convection due to wind mixing is the major process responsible for maintaining the shallow spring and summer mixed layer in which heat is transported downward. For this we follow the algorithm outlined by Thompson (1976, 1977), based on Kraus and Turner (1967), in which a fraction of the turbulent kinetic energy (TKE) generated by the wind is used to mix the water and increase its potential energy. In Brenner et al. (1991) the expression for TKE was based on the surface wind. Since the MRF

provides the surface wind stress, here we use the appropriate alternative expression. TKE is assumed to decay downward (Elsberry et al., 1976) and is given by

$$TKE = \rho\, u_*^3\, \Delta t\, \exp(-z/D) \qquad (3)$$

where $u_* = (\tau / \rho)^{1/2}$ is the friction velocity of the water, τ is the wind stress, Δt is the time step, and D is a dissipation depth scale. TKE is compared to the increase in potential energy required (RPE) to overcome bouyancy and entrain the next lowest layer,

$$RPE = 0.5\, g\, z_n\, (\rho_{n+1} - \rho_n)\, \Delta z \qquad (4)$$

where g is gravity, n is the layer index, and Δz is the layer thickness. The derivation of (4), which is appropriate for a model with layers of equal thickness, is given in Brenner et al. (1991). In the present version of the model, weighting factors have been included in the expression for RPE to allow for layers with varying thickness. If TKE exceeds RPE, then the next layer is entrained, the mixed layer temperature and salinity are set to the weighted averages of the values in layer n+1 and the n layers above, and TKE is decremented by RPE. The process continues until TKE is completely used up. If RPE < TKE then layer n+1 is only partially entrained. If RPE < 0 (i.e., statically unstable) we follow Gill and Turner (1976) and assume that 85% of the

potential energy released by free convection is dissipated in the mixed layer and 15% of RPE is added to TKE.

All other subgrid scale mixing is represented by a background eddy diffusion term

$$\overline{w'T'} = - K_T \frac{\partial \bar{T}}{\partial z} \qquad (5)$$

$$\overline{w'S'} = - K_S \frac{\partial \bar{S}}{\partial z} \qquad (6)$$

where the diffusion coefficients for heat and salt, K_T and K_S, can be functions of depth. Here we assume $K_T = K_S = 10^{-6}\ m^2 s^{-1}$.

Finally, in the numerical scheme, diffusion is computed explicitly as part of the time step while free and forced convection are applied as adjustments after the temperature and salinity have been updated by the time scheme.

2.2 Vertical advection by the mean flow

In this study it is assumed that the currents are forced by the wind only and that these currents are in steady state balance with the wind. Since our main interest is in the vertical heat balance of the water column, we consider only the effects of vertical advection which is induced by the curl of the wind stress. The effects of horizontal advection are negelected at this stage.

Open ocean points

At open ocean points, the vertical velocity depends upon the horizontal divergence of the Ekman transport. Assuming the currents in the mixed layer are uniform in the vertical, then the vertical velocity at the base of the mixed layer is obtained by mass conservation from the vertical component of the curl of the wind stress

$$W_h = - \frac{1}{\rho f} \left(\frac{1}{\cos\phi} \frac{\partial \tau_\phi}{\partial \lambda} - \frac{\partial \tau_\lambda}{\partial \phi} + \frac{\tau_\lambda}{\cos\phi \sin\phi} \right) \qquad (7)$$

where λ and ϕ are longitude and latitude respectively. The minus sign on the right hand side of (7) is necessary since z is defined as postive downward. Below the mixed layer the vertical velocity is assumed to linearly decay with depth from W_h to zero at the bottom of the model.

Coastal points

At points adjacent to coasts, the vertical velocity (upwelling and downwelling) depends upon the component of the local wind stress parallel to the coastline. Once again from mass conservation considerations, the vertical velocity at the base of the mixed layer is given by

$$W_h = - \frac{\tau_y}{\rho f L} \qquad (8)$$

where τ_y is the component of the wind stress parallel to the

coast and L is the width of the region over which coastal upwelling is assumed to be important. Here we set L = 20 km.

2.3 Penetrative radiation

The penetrative component of solar radiation is the only source of internal heating in the water column. It is assumed to decay rapidly with depth. Here we use the double exponential fit to the decay derived by Simpson and Paulson (1977)

$$I(z) / I_0 = R \exp(-z/\mathcal{E}_1) + (1-R) \exp(-z/\mathcal{E}_2) \qquad (9)$$

where I_0 is the surface value. The two exponentials represent the decay of the red and green ends of the spectrum, respectively. Here we use values for Jerlov (1976) water type I with R = 0.58, $\mathcal{E}_1$ = 0.35 m, and $\mathcal{E}_2$ = 23 m.

2.4 Boundary condition

In addition to the solar radiation (I_0), thermal forcing of the model at the surface is provided by longwave cooling (R_B), latent heat flux (H_L), and sensible heat flux (H_S). The salt flux at the surface depends upon the excess of evaporation ($E = H_L/L_v$) over precipitation (P) where L_v is the heat of vaporization. Forced convection depends upon the surface wind stress. For the idealized forcing cases presented in section 3, the heat fluxes and wind stress are specified. For the coupled model experiments in section 4, the fluxes and wind

stress are taken as the averages over the previous 12 hours of the values computed by the MRF while the precipitation is taken as the amount accumulated over the previous 12 hours.

At $z = 0$, the heat flux boundary condition is

$$- \rho C_p \overline{w'T'} = H_0 = - I_0 + R_B + H_L + H_S \qquad (10)$$

where we have used the convention that a positive flux is directed upward. The surface boundary condition on salinity is

$$- \rho \overline{w'S'} = (P - E) S_0 \qquad (11)$$

where S_0 is the surface salinity. The wind stress is accounted for by (3).

For the lower boundary conditions we tested both a no flux condition as well keeping T and S fixed. The bottom of the model z_B is placed at or below the base of the seasonal thermocline where temporal variations are small. For the time scales of interest here (several days to weeks) the results are rather insensitive to the choice of the lower boundary condition. Unless otherwise noted, we keep T and S at the bottom fixed at their initial values.

3. Model tests with idealized forcing

Before coupling the mixed layer model to the MRF it is of

interest to test the performance of the model under various idealized forcing conditions. This also provides a convenient way to compare our model to other mixed layer models that have appeared in the literature. While there are no standard tests to which various models have been subjected, there have been several efforts, most notably by Thompson (1976), by Martin (1985), and by McCormick and Meadows (1988), to compare several models within a single study.

Martin (1985) has classified the various mixed layer models into two basic categories: differential and bulk. In the latter, the mixed layer is treated as a single well defined layer over which the appropriate equations are integrated while in the former the equations are used in their basic form and not integrated over the mixed layer. The higher order closure models (e.g. Mellor and Yamada, 1982) are of the differential type while our model as well as the models of Kraus and Turner (1967), Denman (1973), Pollard et al. (1973), Niiler (1975), Elsberry et al. (1976), Garwood (1977), Thompson (1976), Price et al. (1986), and Woods and Barkmann (1986) are examples of the bulk type. All of the bulk models can trace their development back to the work of Kraus and Turner (1967) or Pollard et al. (1973) which differ only in their assumptions of the mechanism responsible for entrainment. In Kraus-Turner type models entrainment and mixed layer deepening are directly proportional to the wind energy imparted to the water while in the Pollard type models mixed layer deepening is driven by shear instabilites

generated at the base of the mixed layer. As noted in the previous section, our model is of the Kraus-Turner type.

Our model was tested by subjecting it to the three types of forcing used by Martin (1985): wind mixing, surface heating, and surface cooling. In all cases the water column from the surface to 200 m was divided into 100 equal thickness layers and the time step was taken as one hour. For the wind deepening experiments the inital conditions were SST of 24°C, uniform lapse rate of $0.05^{\circ}C\ m^{-1}$, and a constant salinity of 35 ppt. The surface heat and salt fluxes were zero. The model was run for five days with wind stress values of 0.1, 0.4, and 1.6 $N\ m^{-2}$. For the surface heating experiments the initial temperature profile consisted of a 100 m deep mixed layer with a temperature of 19° C and a uniform lapse rate of $0.05^{\circ}C\ m^{-1}$ below. The model was run for two days with a constant wind stress of 0.1 $N\ m^{-1}$ and a net surface heat flux of 72.6, 290.7, and 1162.8 $W\ m^{-2}$. For the cooling experiments, the same initial profile from the wind deepening runs was used and the model was run for 120 days subjected to a net surface cooling of 48.4, 96.8, and 145.2 $W\ m^{-2}$.

The results of these tests are summarized in Table 1. For comparison we have also listed the results from Martin (1985) for the Mellor and Yamada (1982) level 2.5 model, the Niiler (1975) model, and the Garwood (1977) model. From the Table it can be seen that our model compares favorably with the other models for all three forcing regimes. Further discussion of the performance

of the various models can be found in Martin (1985).

Table 1. Comparison of Mixed Layer Depths from Various Models for Idealized Forcing Experiments

Experiment	MY	Niiler	Garwood	Brenner
	Mixed Layer Depth (m)			
Wind mixing (H_0=0 W m^{-2}, 5 days)				
τ = 0.1 N m^{-2}	18	27	26	29
τ = 0.4	39	54	51	55
τ = 1.6	76	108	103	101
Surface heating (τ = 0.1 N m^{-2}, 2 days)				
H_0 = -72.6 W m^{-2}	26	17	33	35
H_0 = -290.7	14	4	14	11
H_0 = -1162.8	8	1	4	3
Surface cooling (τ= 0.1 N m^{-2}, 120 days)				
H_0 = 48.4 W m^{-2}	73	101	90	97
H_0 = 96.8	103	127	117	117
H_0 = 145.2	127	150	140	137

A complete comparison of model performance should also include SST which is unfortunately omitted by Martin (1985). A similar exercise of model comparison for idealized forcing was conducted by McCormick and Meadows (1988), although their tests focused on conditions for a shallow inland sea (i.e., the Great Lakes). We configured our model to conform with their experiments and found the results for both SST and mixed layer depth to compare favorably with the other bulk models that they tested. We note however that there appears to be an error in the results

they reported for two of the heating experiments. One additional point not mentioned in either of the above studies is that the heat content (i.e., integrated temperature) of the water column should be conserved in the wind mixing experiments which have no net surface heat flux. This was indeed the case for our model.

In deciding upon a final configuration of the mixed layer model to be coupled to the MRF, one must choose appropriate vertical and temporal resolution. To this end we repeated the middle experiment from each of the three idealized forcing regimes with various vertical grid spacings and time steps. The results of the vertical resolution tests are summarized in Table 2. Tests were conducted for 200, 100, 50 30, 20 and 10 equal thickness layers (corresponding to Δz of 1, 2, 4, 6.67, 10, and 20 m) and for 30 variable thickness layers (denoted 30V) where the layer thicknesses increased smoothly from 2.37 m at the top to 10.96 m at the bottom. In all cases, the 30V results compared favorably with the 200 layer run so that 30V was chosen as the resolution of the model to be coupled to the MRF. We also tested the sensitivity of the model to the size of the time step. The results for steps of 1, 3, 6, 12, and 24 hr were virtually indistinguishable.

We conclude this section with a final experiment designed to test the ability of the mixed layer model to simulate the effects of the diurnal cycle of solar heating. Woods and Barkmann (1986) found that in order to properly simulate the annual range of mixed layer temperatures

Table 2. Effects of Vertical Resolution on Mixed Layer Depth and Temperature

Experiment	ML depth (m)	ML temperature (°C)
Wind mixing (H_0 = 0, τ = 0.4 N m^{-2}, 5 days)		
K = 200 layers	56.5	22.61
K = 100	55.0	22.60
K = 50	54.0	22.59
K = 30	50.0	22.58
K = 30V	51.0	22.59
K = 20	45.0	22.55
K = 10	50.0	22.49
Surface heating (H_0 = -290.7 W m^{-2}, τ = 0.1 N m^{-2}, 2 days)		
K = 200	10.5	20.09
K = 100	11.0	20.00
K = 50	10.0	19.88
K = 30	10.0	19.76
K = 30V	9.6	19.98
K = 20	5.0	24.43
K = 10	10.0	19.46
Surface cooling (H_0= 96.8 W m^{-2}, τ = 0.1 N m^{-2}, 30 days)		
K = 200	67.5	21.43
K = 100	67.0	21.43
K = 50	66.0	21.43
K = 30	63.3	21.42
K = 30V	63.4	21.42
K = 20	65.0	21.40
K = 10	50.0	21.37

and depths, a mixed layer model must be capable of resolving the diurnal cycle. They showed that this could be accomplished through the use of a small enough time step or by including a suitable parameterization of the diurnal variation of the solar zenith angle. This must be weighed against the possibility of introducing excessive noise into the predicted SST field when using too small a time step for coupling as found by Elsberry et

al. (1984). This experiment was similar to the net surface heating experiments described above. Initial conditions consisted of a 30 m deep mixed layer with a temperature of 20°C, a constant lapse rate of 0.05°C m^{-1} below the mixed layer, and a constant salinity of 35 ppt at all levels. The model was run for five days with a constant cooling of 100 W m^{-2} and a wind stress of 0.1 N m^{-2}. Three representations of diurnal heating (and associated time step) were considered with the assumption of equal day and night: (i) a full diurnal cycle with $I_0 = -200\ \pi \cos(\Omega t)$ during the day and zero at night, where t is time of day (t = 0 at noon) and $\Omega = 2\pi$/day, with a time step of 1 hr; (ii) I_0 = -400 W m^{-2} during the day (daytime average of the heating function in (i)) and zero at night with a time step of 12 hr; and (iii) I_0 = -200 W m^{-2} during both day and night (daily average heating) also with a time step of 12 hr (although our previous results showed that the size of the time step in this case is not important). In all three cases the net heating over a full day is the same.

The results for this experiment are shown in Figure 1 where we present the evolution of the mixed layer temperature and depth over the five days of the simulation. Case (i) is given by the solid line, case (ii) by the large dashed line, and case (iii) by the small dashed line. From the figure we can see that the use of the daytime average heating (case (ii)) provides a reasonable approximation of the full diurnal cycle. The diurnal range of SST (defined as the difference between the maximum

and the following minimum) in case (ii) is only 0.06°C less than in case (i) while the difference in the maximum daytime temperature between the two cases is less than 0.08°C and the difference in the daily minimum between the two cases is less than 0.02° C. The diurnal variation in the mixed layer depth is also reasonably reproduced by case (ii) as compared to the full diurnal cycle although during the day it is about 3 m too deep thus explaining the slightly lower temperature. In contrast to this, case (iii) by definition has no diurnal range. SST in case (iii) is always less than the minimum of cases (i) and (ii) and it is as much as 0.35°C less than the maximum daytime temperature of case (i). Also the mixed layer remains too deep in case (iii) and never gets shallower than 25 m. In view of these results we felt that the use of a 12 hr time step with appropriately averaged surface fluxes was a reasonable choice for coupling of the MRF and the mixed layer model.

4. Coupled model

In this section we describe the method of coupling the mixed layer model to the MRF and the results of the preliminary experiments run with the coupled model. Two types of experiments, designated as one way and two way interaction, were run. In the former the atmospheric fluxes were used to force the ocean model but the predicted SST field was not fed back into the MRF and thus the atmosphere could not respond to the SST changes. In the two way interaction experiments, the models were fully coupled

and the updated SST field was returned to the MRF after each ocean model time step for subsequent use in the computation of the surface fluxes.

4.1 Coupling strategy

In coupling the mixed layer model to the MRF we attempted to keep the ocean model modular and independent and to introduce as few changes as possible in the existing MRF code. The physical interaction between the atmosphere and the oceans occurs through the surface fluxes which lead to the exchange of heat, mass, and momentum across the air-sea interface. In this repsect, the most logical place to couple the MRF and the ocean model would be in the MRF's planetary boundary layer (PBL) scheme. However two important factors weighed against this choice. First, it would require significant reprogramming of several of the PBL subroutines, and second, it would lead to synchronous coupling of the two models at every MRF time step (roughly every twenty minutes) which is more frequent than necessary.

In the previous section we found that the mixed layer model reasonably simulated the diurnal cycle with a 12 hr time step and appropriately averaged surface fluxes. Furthermore, Elsberry et al. (1984) suggested that coupling of atmospheric and oceanic models might best be accomplished at an interval of one day (i.e. by using the daily averaged surface fluxes to drive the ocean model) in order to reduce the noise in the predicted SST field. Considering these two factors, we decided to couple the

models at 12 hr intervals. This allowed us to take advantage of the MRF job stream in which the model is executed in 12 hr forecast segments. During each of these forecast segments, the MRF accumulates the wind stress and all of the surface fluxes required for the ocean model except for the solar heating. Accessing the fluxes and the wind stress was fairly straightforward as they all are stored in arrays which are located in common. The average solar flux had to be obtained directly from the radiation routines. The ocean model was run by simply adding a subroutine call near the end of the MRF's main program. In the one way interaction experiments, the predicted SST field was kept internal to the ocean model. In the two way interaction experiments the predicted SST field was passed back to the MRF through the normal updating of the surface fields via the surface temperature array TSEA in preparation for the next forecast segment.

Following is a summary of the changes and additions made to the MRF code.

Changes

1. In the surface merge program (ASFC) a two dimensional array was added to hold the correction for topography applied to the initial SST field. This array is written to UNIT 93 and read back by the ocean model.

2. In the MRF main program two surface field arrays were added to hold the net longwave and net shortwave fluxes at the surface. Near the end of the main program a series of three subroutine

calls were added to run the ocean model. The order of these calls is AVSFLX, OCEAN, AVSFLX.

3. In subroutine WR2DDF a two dimensional surface field array was added to hold the net downward shortwave flux at the surface. Several lines of code were added to compute the net flux as the difference between the downward and upward fluxes and the net field is written into UNIT 90 for use by the ocean model.

Additions

1. SUBROUTINE AVSFLX is called once before and once after the ocean model. On the first call, this subroutine converts the accumulated surface fluxes and wind stress into 12 hr averages and passes these fields through the ROWSEP subroutine (Gaussian grid rearrangement). On the second call, the subroutine "unaverages" the fluxes and restores the grid arrangement of these fields (through subroutine ROW1NS) for subsequent use by the MRF.

2. SUBROUTINE OCEAN is the driving routine for the ocean model and is the interface to the MRF. All other subroutines used by the ocean model are included in the program module (data set) which contains OCEAN.

4.2 Experiments and results

Since the mixed layer model is one dimensional, it was fairly straighforward to adapt it to run on the Gaussian grid of the MRF. For the experiments reported below, we ran the model at a resolution of T62 which has a latitude longitude grid of 94 X

192 points. Furthermore, we did not consider any points poleward of 60° latitude or points at which the SST was less than 0° C since the mixed layer model does not include a parametrization of sea ice. We began with a one way interaction experiment run for 10 days starting from 00Z on 15 March 1991. During the initial experiment a history file containing the surface fluxes at 12 hr intervals was generated. These fluxes were used to provide the surface forcing for additional one way experiments without having to run the MRF each time.

Our primary intention in this phase of the model development was to demonstrate the capabilities, stability, and potential usefulness of the coupled model. We therefore made only a minimal effort to tune the model and verification of the coupled forecasts was limited mainly to comparisons between the analyzed (i.e., "observed") and predicted changes of SST. Nevertheless, the experimental forecasts and the tuning procedure did accomplish the goal of demonstrating the model's capabilities. They also helped identify the strengths and weaknesses of the coupled model and provided some insight into defining various directions for further model improvement and development. The tuning was done by running a series of one way experiments, all from the same initial time, but with different values of various adjutable parameters and switches in the mixed layer model. As noted above, these one way experiments could be executed quickly and easily without the need for rerunning the MRF each time.

At this stage we must comment on the specification of initial conditions for the ocean model. A full ocean general circulation model requires initial fields of tempertaure, salinity, and horizontal velocity components on the various model levels as well as sea level height. Due to the simplicity of the mixed layer model (i.e., a one dimensional model that neglects horizontal advective processes) we minimally require a temperaure profile at each grid point to initialize the model. At most points salinity effects are of secondary importance (the most notable exception is at high latitudes where salinity plays a major role in controlling the static stability of the water column), although it is desirable to include salinity profiles if available. Unfortunately there is no operationally available ocean data assimilation system that can provide the necessary profiles on a daily basis. We can however construct reasonable initial fields by combining the operational SST analyses with climatological subsurface information. Furthermore, experience has shown that mixed layer models, which in effect describe the ocean's response to local surface forcing, generate their own "preferred" or "quasi-balanced" profiles within a few days. Thus our initial fields were constructed as follows. For temperature we took the operational SST analysis from the initial time and assumed that it also represented the mixed layer temperature. The initial mixed layer depths were specified as a function of latitude only and taken from the monthly zonal means of Gallimore and Houghton (1990). Below the mixed layer we assumed a linear

lapse rate of 0.05°C m^{-1}. The initial salinity profiles were also specified as a function of latitude following Pollard et al. (1983). In the mixed layer salinity was given by $S = 35 - 3 \sin^4\phi$ while below the mixed layer it was set to a constant value of 35 ppt.

As noted above, we began by running a series of one way experiments designed to test and tune the mixed layer model. The main purpose here was to arrive at tentative values for the adjustable parameters which include the turbulence dissipation depth (D in eq. (3)), and the minimum allowable mixed layer depth, h_{min}. The latter is designed to control excessive surface temperature increases which could occur in low latitudes where the net surface heating reaches values of several hundred W m^{-2}. Values of D = 100 m and h_{min} = 25 m were found to give satisfactory results. One could conceivably tune these values for each individual grid point, however this would be beyond the scope of the current study and there is no guarantee that such fine tuning would be appropriate under other forcing conditions. Thus the above values were specified globally. We also compared forecasts with and without salinity and found that the inclusion of salinity improved the forecast especially in higher latitudes.

Upon being satisfied that the one way model was behaving reasonably well, we proceeded to the full two way experiment. The results of the two way forecast are shown in Figure 2 where we have plotted the 5 day predicted (upper panel) and observed (lower panel) SST changes. Figure 3 shows the 10 day predicted

and analyzed changes. In both figures the contour interval is 0.2 °C and regions of cooling are shaded. Considering the relative simplicity of both the ocean model and the specification of the initial conditions, the forecast is remarkably good. The large scale pattern of regions of heating and cooling is predicted quite well although the predicted changes are smaller and smoother than observed. We note however that many of the smaller scale features in the observed field may very well be artifacts of the analysis scheme and not physically based. It is also interesting to note that the model did reasonably well even in areas where ocean dynamics are expected to be as important as mixed layer processes (i.e., in the tropics and in regions of major western boundary currents such as the Gulf Stream). Some of the notable successes of the forecast are: (1) the band of heating along the equator in the eastern Pacific flanked by a region of cooling to the northwest; (2) the band of heating extending northeastward from the Caribbean across the North Atlantic flanked by large regions of cooling to the northwest and to the southeast; (3) the general heating trend across the Arabian Sea and the Bay of Bengal; (4) the region of cooling to the east of Japan; and (5) the distribution of heating and cooling along the north and east coasts of Australia. The two most noticable deficiencies of the model are: (1) its general inability to simulate the cooling across much of the Southern hemisphere midlatitudes (especially in the eastern Pacific and in the southwestern Indian Ocean); and (2) its inability to simulate

the cooling along the west coasts of North and South America. It has been suggested that the former problem might be due to an underestimate of cloudiness by the MRF in the Southern hemisphere (Campana, private communication). The latter problem indicates that the model's treatment of coastal upwelling along eastern boundaries is probably inadequate.

In Table 3 we give the verification scores of the one way, two way, and persistence forecasts in terms of the RMS error of the day 10 forecast (i.e,. forecast - analysis) in 20 latitude bands. The results show that both the one way and two way forecasts beat persistence in all latitude bands considered.

Table 3. Verification scores of the day 10 SST forecasts

Latitude band	RMSE (°C)		
	One way	Two way	Persistence
40 - 60 N	0.293	0.292	0.375
20 - 40 N	0.368	0.366	0.425
0 - 20 N	0.334	0.312	0.345
0 - 20 S	0.386	0.376	0.395
20 - 40 S	0.397	0.393	0.411
40 - 60 S	0.298	0.300	0.368

Furthermore, allowing the updated SSTs to feed back into the atmospheric model (i.e., the two way interaction case) leads to modest improvements in the predicted SST field.

5. Conclusion and recommendations

The results presented in this report represent a first step in the development of a coupled ocean-atmosphere model for use in medium to extended range forecasting. Our main purpose was to demonstrate the capabilities and potential usefulness of such a model. The results of preliminary experiments indicate that the coupled model is capable of producing forecasts of SST which are better than persistence and therefore superior to the current operational "no change" forecasts. Furthermore, testing of the model has given us insight into various directions for improving the ocean model. The coupled model could also serve as a useful tool in diagnosing the strengths and weaknesses of the MRF produced surface fluxes. With this in mind we recommend the following topics for the next phase of the model development:

(1) Run additional experiments (higher resolution and additional initial conditions) to firmly establish the model's skill.

(2) Analyze the atmospheric response to the use of predicted SSTs.

(3) Improve the ocean model by adding a rudimentary representation of ocean dynamics.

(4) Improve the method of constructing initial conditions by

using mixed layer depths and profiles below the mixed layer based on climatology with more spatial variability (i.e. function of longitude as well as latitude).

Acknowledgments

I would like to thank UCAR for funding this work through its visiting scientist program. I would also like to thank Drs. E. Kalnay and M. Kanamitsu of the Development Division for hosting me at NMC and for helping make my visit both enjoyable and productive. My appreciation is also extended to all of the other people at NMC who helped guide me through the bureacracy, the computer systems, and the MRF. Dr. Mark Iredell ran the final T62 experiment and produced the maps presented in this report.

References

Brenner, S., Z. Rozentraub, J. Bishop, and M. Krom, 1991. The mixed-layer/thermocline cycle of a persistent warm core eddy in the eastern Mediterranean. Dyn. Atmos. Oceans, **15**, 457-476.

Bryan, K., S. Manabe, and R.C. Pacanowski, 1975. A global ocean-atmosphere climate model. Part II: the oceanic circulation. J. Phys. Oceanogr., **5**, 30-46.

Denman, K.L., 1973. A time dependent model of the upper ocean. J. Phys. Oceanogr., **3**, 173-184.

Elsberry, R., T.S. Fraim, and R.N. Trapnell, 1976. A mixed layer model of the oceanic thermal response to hurricanes. J. Geophys. Res., **81**, 1153-1161.

Elsberry, R.A., S.A. Sandgathe, and F.J. Winninghoff, 1984. Short-term oceanic response predicted by amixed layer model forced with a sector atmospheric model. J. Phys. Oceanogr., **14**, 79-91.

Gallimore, R.G. and D.D. Houghton, 1990. Simulation of ocean temperature and heat storage from a GCM coupled to a variable depth upper ocean. J. Phys. Oceanogr., **20**, 1312-1332.

Garwood, R.W. (1977). An oceanic mixed layer model capable of simulating cyclic states. J. Phys. Oceanogr., **7**, 455-471.

Gill, A.S. and J.S. Turner, 1976. A comparison of seasonal thermocline models with observations. Deep Sea Res., **23**, 391-401.

Jerlov, N.G., 1976. Marine Optics. Elsevier, Amsterdam, 141 pp.

Kraus, E.B. and J.S. Turner, 1967. A one dimensional model of the seasonal thermocline. II: the general theory and its consequences. Tellus, **19**, 98-106.

Martin, P.J., 1985. Simulation of the mixed layer at OWS November and Papa with several models. J. Geophys. Res., **90**, 903-916.

McCormick, M.J. and G.A. Meadows, 1988. An intercomparison of four mixed layer models in a shallow inland sea. J. Geophys. Res., **93**, 6774-6788.

Mellor, G.L. and T. Yamada, 1982. Development of a turbulence closure model for geophysical fluid problems. Rev. Geophys., **20**, 851-875.

Michaud, R., 1990. Extended memory of initial conditions in long range forecasts of the January 1983 atmospheric circulation. J. Climate, **3**, 461-482.

Niiler, P.P., 1975. Deepening of the wind mixed layer. J. Mar. Res., **33**, 405-422.

Owen, J.A. and T.N. Palmer, 1987. The impact of El Nino on an ensemble of extended range forecasts. Mon. Wea. Rev., **115**, 2103-2117.

Pollard, R.T., M. L. Batteen, and Y.-J. Han, 1983. Development of a simple upper-ocean and sea-ice model. J. Phys. Oceanogr., **13**, 754-768.

Pollard, R.T., P.B. Rhines, and R.O.R.Y. Thompson, 1973. The deepening of the wind mixed layer. Geophys. Fluid Dyn., **3**, 381-404.

Price, J.F., R.A. Weller, and R. Pinkel, 1986. Diurnal cycling: observations and models of the upper ocean response to diurnal heating cooling and wind mixing. J. Geophys. Res., **91**, 8411-8427.

Ranelli, P.H., R.H. Elsberry, C.-S. Liou, and S.A. Sandgathe, 1985. Effects of varying sea-surface temperature on 10-day atmospheric model forecasts. In: J.C.J. Nihoul (Editor), Coupled Ocean-Atmosphere Models. Elsevier, Amsterdam, pp. 675-696.

Simpson, J.J. and C.A. Paulson, 1977. Irradiance measurements in the upper ocean. J. Phys. Oceanogr., **7**, 952-956.

Thompson, R.O.R.Y., 1976. Climatological numerical models of the surface mixed layer of the ocean. J. Phys. Oceanogr., **6**, 496-503.

Thompson, R.O.R.Y. 1977. Reply. J. Phys. Oceanogr., **7**, 470-471.

Woods, J.D. and W. Barkmann, 1986. The response of the upper ocean to solar heating. I: The mixed layer. Quart. J. R. Met. Soc., **112**, 1-27.

List of Figures

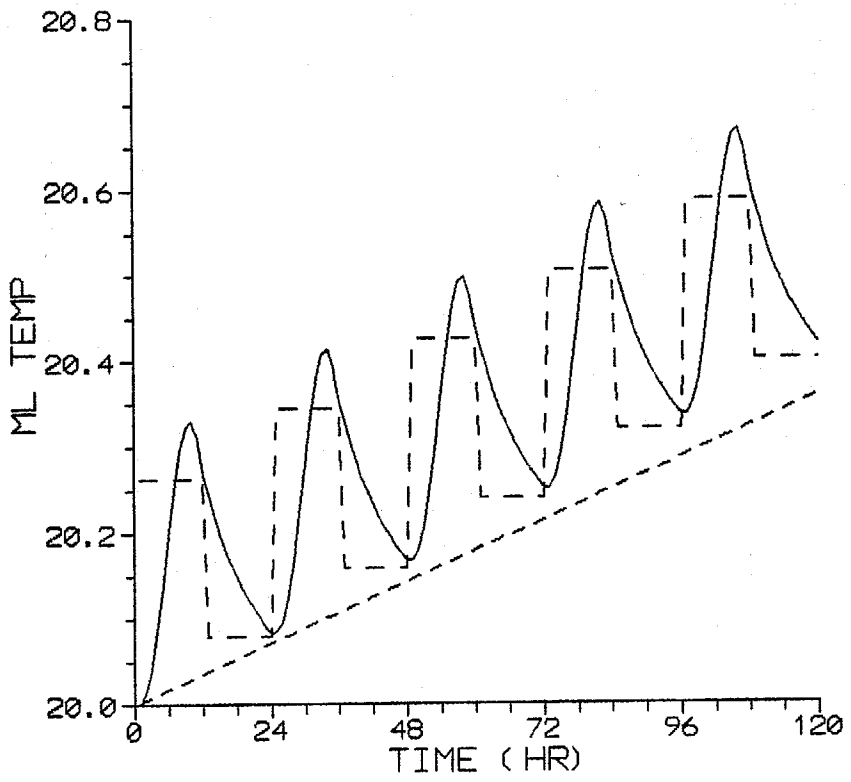
ML TEMP
20.8
20.6
20.4
20.2
20.0
0
24
48
72
96
120
TIME (HR)

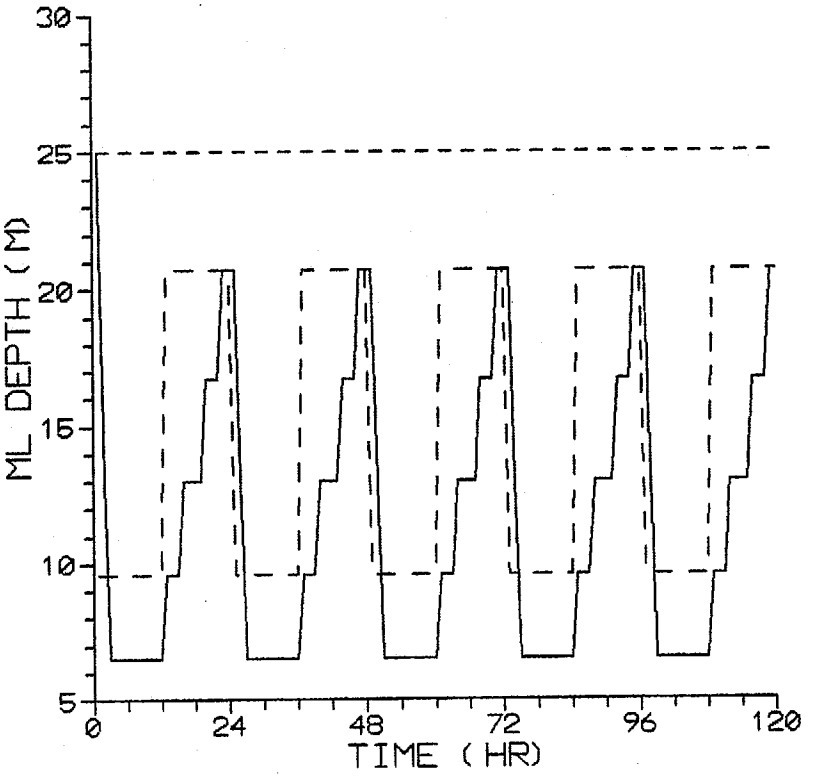
ML DEPTH (M)
30
25
20
15
10
5
0
24
48
72
96
120
TIME (HR)

5–DAY COUPLED FORECASTS OF SST CHANGES FROM MARCH 15, 1991

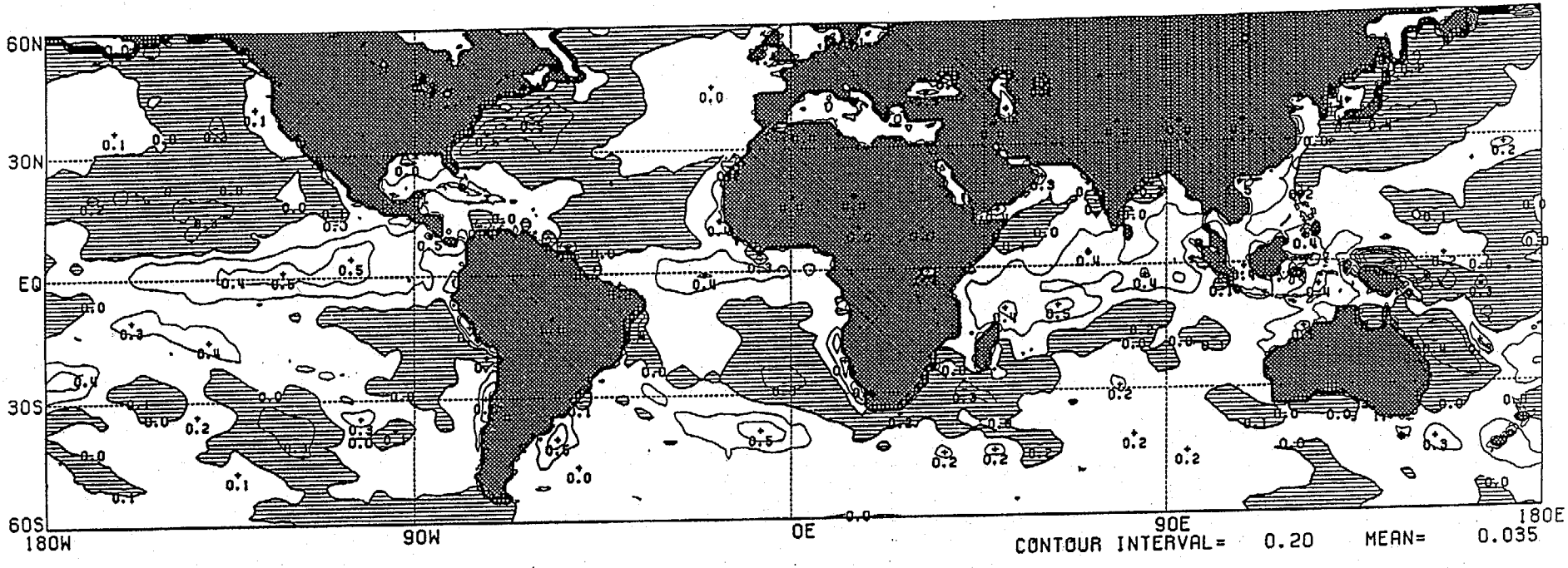

ANALYZED 5–DAY SST CHANGES FROM MARCH 15, 1991

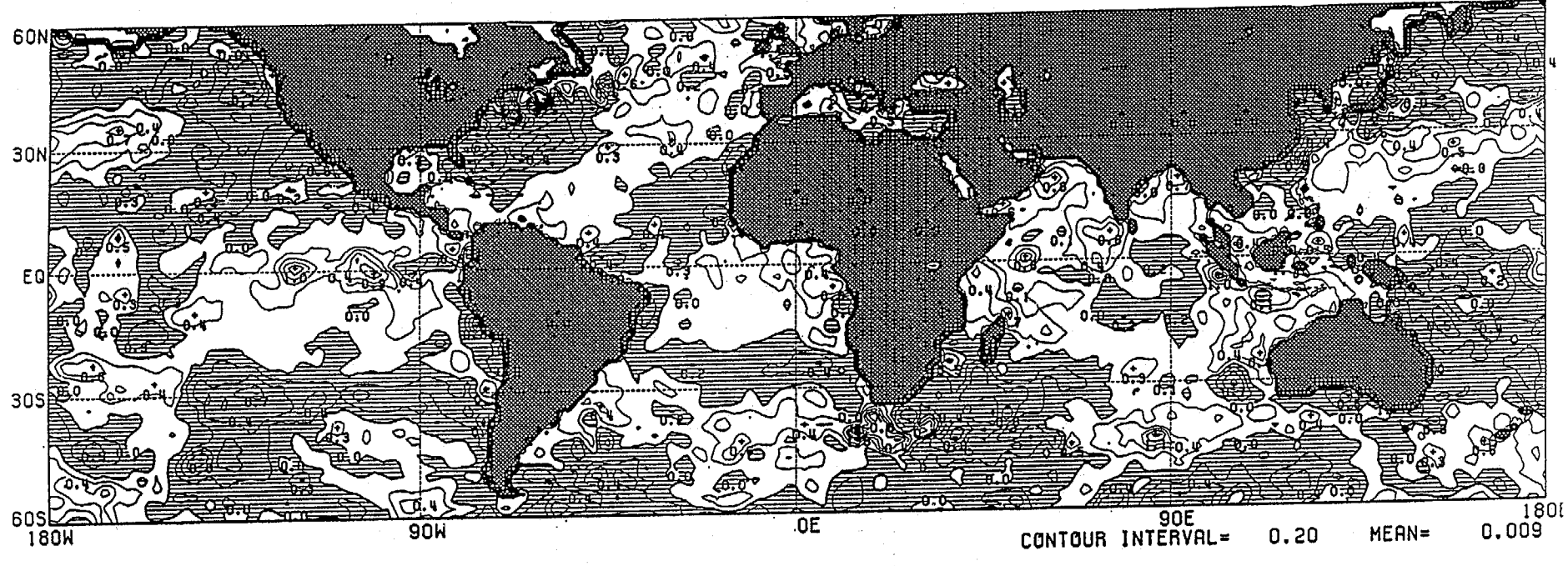

10–DAY COUPLED FORECAST OF SST CHANGES FROM MARCH 15, 1991

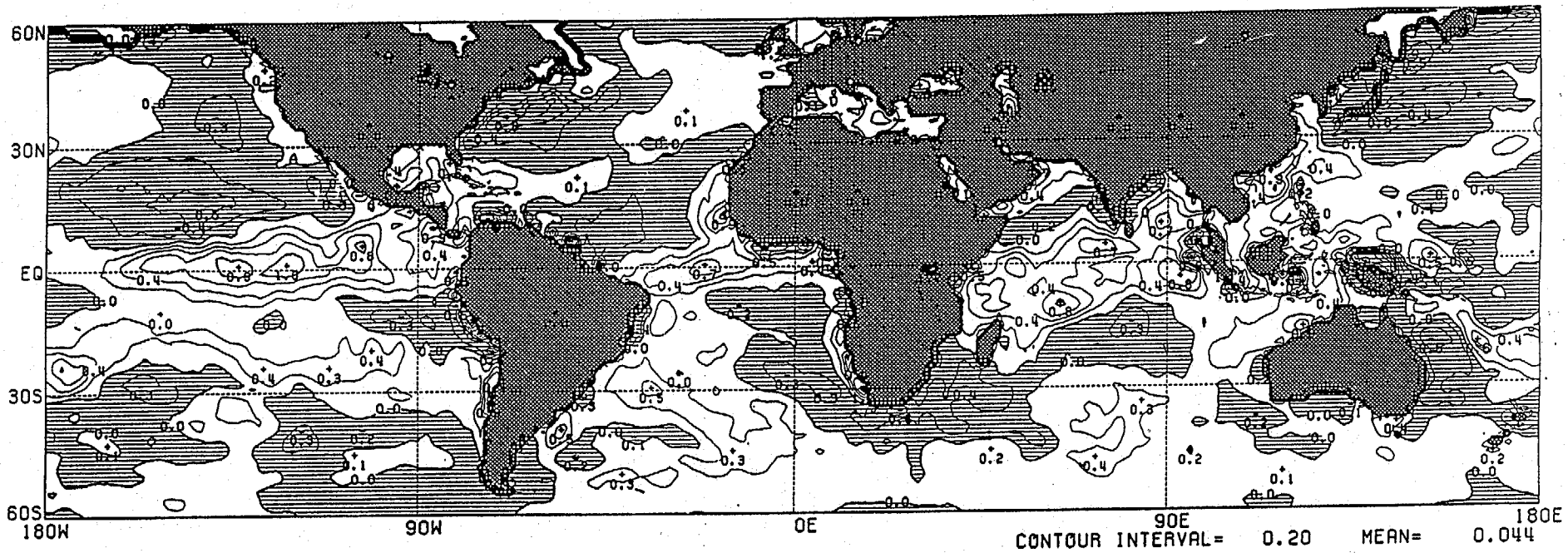

ANALYZED 10–DAY SST CHANGES FROM MARCH 15, 1991